# Low-Temperature MCD Studies of Low-Spin Ferric Complexes of Tetramesitylporphyrinate: Evidence for the Novel $(d_{xz},d_{yz})^4(d_{xy})^1$ Ground State Which Models the Spectroscopic Properties of Heme *d*

**Myles R. Cheesman**[‡] **and F. Ann Walker***

*Contribution from the Centre for Metalloprotein Spectroscopy and Biology,*
*School of Chemical Sciences, University of East Anglia, Norwich NR4 7TJ, Great Britain, and*
*Department of Chemistry, University of Arizona, Tucson, Arizona 85721*

*Received February 1, 1996*[⊗]

**Abstract:** Low-temperature MCD spectra were recorded for the bis 4-(dimethylamino)pyridine (**1**), bis(1-methylimidazole) (**2**), and bis(4-cyanopyridine) (**3**) complexes of ferric tetramesitylporphyrinate. The ground state electronic configuration is formally $(d_{xy})^2(d_{xz},d_{yz})^3$ for both **1** and **2**, but these two complexes give rise to near-infrared porphyrin$(\pi) \rightarrow$ ferric(d) charge transfer bands (NIR-CT) with very different MCD intensities. These intensity differences are correlated with the symmetry imposed on the ferric ion by different relative orientations of the ligand planes in these two complexes. Near perpendicular ligand planes in **1** result in effective 4-fold symmetry at the ferric ion and intense NIR-CT MCD while parallel ligand planes in **2** give rise to relatively weak NIR-CT MCD. Complex **3** has perpendicularly orientated ligands but displays an axial EPR spectrum with unusual *g*-values and anomalously weak MCD transitions not only in the NIR but also across the ultraviolet and visible wavelengths. It is argued that these low intensities are the result of a novel $(d_{xz},d_{yz})^4(d_{xy})^1$ ground state for which the NIR-CT transition is formally symmetry forbidden. Complex **3** thus provides an explanation for the unusual EPR and MCD properties of low-spin ferric forms of heme *d*, which have similar EPR spectra to complex **3**. It is concluded that these properties are a consequence of a reordering of the energies of the ferric d-orbitals by the axial ligands for the porphyrinate complex, or by the macrocycle for chlorin complexes, in each case leading to a predominantly $(d_{xz},d_{yz})^4(d_{xy})^1$ ground state.

## Introduction

It has long been known that the ultraviolet and visible region electronic spectra of hemoproteins are dominated by the $\pi-\pi^*$ transitions of the porphyrin ring.[1,2] The electronic states of the iron mix with those of the porphyrin $\pi$-system making the form of the corresponding Magnetic Circular Dichroism (MCD) spectrum diagnostic of the oxidation and spin state of the metal ion.[3] Additionally, because it is relatively insensitive to vibrational transitions,[4] MCD spectroscopy can be used to observe the electronic transitions of protein-bound hemes in the near-infrared (NIR) region between 1000 and 2500 nm where the absorption spectrum is dominated by vibrational bands. This spectral region has proved especially informative in the case of low-spin ferric hemoproteins because it contains a porphyrin $(\pi) \rightarrow$ ferric (d) $(a_{1u} \rightarrow e_g)$ charge transfer (CT) transition, the wavelength of which varies as a function of the energies of the acceptor d-orbitals. The peak wavelength of the transition is consequently diagnostic of the nature of the axial ligands bound to the ferric ion. The correlation can conveniently be expressed as an "additivity rule" whereby a specific axial ligand is assigned an energy parameter which is independent of the nature of the second ligand. The peak energy of the NIR-CT band is then given simply by the sum of the two appropriate parameters.[3,5] In many cases, the NIR-CT band energy is in itself sufficient to identify the two protein-derived heme ligands. Where ambiguity arises, the EPR spectrum is usually sufficient to resolve the assignment.

A number of proteins have now been shown to contain iron bound in macrocycles which are reduced analogues of the porphyrin structure. Chlorin is the macrocycle of the heme *d* found in hydroperoxidase II and cytochrome *bd* from *Escherichia coli*. Heme $d_1$, an iron dioxoisobacteriochlorin, is a prosthetic group in the nitrite reductases of denitrifying bacteria. These two iron "hydroporphyrins" have $\pi$-systems which are respectively two and four electrons reduced relative to the parent porphyrin structure.[6−8] The small number of completed MCD studies of low-spin ferric heme *d*-containing proteins suggest that the energy of an NIR-CT MCD band does indeed vary with changing axial ligation,[9−12] but more examples are required to determine if this variation is as systematic as has been found

* Address correspondence to this author at the University of Arizona.
‡ Address correspondence to this author at the University of East Anglia.
⊗ Abstract published in *Advance ACS Abstracts,* July 1, 1996.
(1) Gouterman, M. Optical Spectra and Electronic Structure of Porphyrins and Related Rings. In *The Porphyrins*; Dolphin, D., Ed.; Academic Press: New York, 1978; Vol. III, pp 1−165.
(2) Adar, F. Electronic Absorption Spectra of Hemes and Hemoproteins. In *The Porphyrins*; Dolphin, D., Ed.; Academic Press: New York, 1978; Vol. III, pp 165−209.
(3) Cheesman, M. R.; Greenwood, C.; Thomson, A. J. *Adv. Inorg. Chem.* **1991**, *36*, 201−255.
(4) Nafie, L. A.; Keiderling, T. A.; Stephens, P. J. *J. Am. Chem. Soc.* **1976**, *98*, 2715−2723.

(5) Gadsby, P. M. A.; Thomson, A. J. *J. Am. Chem. Soc.* **1990**, *112*, 5003−5011.
(6) Timkovich, R.; Cork, M. S.; Taylor, P. V. *J. Biol. Chem.* **1984**, *259*, 1577−1585.
(7) Timkovich, R.; Cork, M. S.; Gennis, R. B.; Johnson, P. Y. *J. Am. Chem. Soc.* **1985**, *107*, 6069−6075.
(8) Wu, W.; Chang, C. K. *J. Am. Chem. Soc.* **1987**, *109*, 3149−3150.
(9) Peng, Q.; Peterson, J. *FEBS Lett.* **1994**, *356*, 159−161.
(10) Cheesman, M. R.; Hiner, A.; Greenwood, C.; Thomson, A. J. Unpublished data.
(11) Peng, Q. Ph.D. Thesis, University of Alabama, 1994.
(12) Peng, Q.; Timkovich, R.; Loewen, P. C.; Peterson, J. *FEBS Lett.* **1992**, *309*, 157−160.

for ferric porphyrins.  The intensities of the NIR-MCD spectra of low-spin ferric hydroporphyrins are significantly lower than those found for analogous iron−porphyrin species.  An MCD study of nitrite reductase failed to detect any NIR-CT bands from heme $d_1$ against the background of intense bands from the $c$-type heme also present.[13]  The low-spin ferric forms of heme $d$ and of heme $d_1$ both give unusual EPR spectra which suggest atypical electronic properties.

The intensity of the NIR-CT MCD band of "normal" low-spin ferric porphyrins is governed by the symmetry at the ferric ion, which is largely determined by the nature and orientation of the axial ligands.[14]  It has been suggested that the weak NIR-CT MCD bands of low-spin ferric chlorins result from the loss of the 4-fold symmetry of the macrocyclic $\pi$-system which causes a rhombicity *at the ferric ion* greater than is encountered with ferric porphyrins.[11,12]  However, such an interpretation does not find support in data reported for other modified porphyrins.

The chromophore of heme $a$ differs from that of heme $b$ by the addition of a formyl moiety at the periphery of the porphyrin ring.[15]  This change removes the $xy$ equivalence and is sufficient to substantially perturb $\pi$–$\pi^*$ transitions localized on the macrocycle.  Distinctive electronic spectra at UV−visible wavelengths result.[16]  However, EPR spectra, which involve transitions localized on the ferric ion, appear to be markedly insensitive to the change from heme $b$ to heme $a$ but do respond to the nature of the axial ligands.  An example of this is provided by two well-characterized structurally related terminal oxidases:  Both heme $a$ in cytochrome oxidase and heme $b$ in cytochrome $bo$ are found in the low-spin ferric form.  The high structural similarity between the two proteins is such that these two hemes are ligated by comparably oriented histidine residues.[17]  Although the UV−visible electronic spectra from the two sites are extremely distinctive, they give rise to virtually identical EPR signals and their NIR-CT MCD bands are comparable in energies, bandshapes, and intensities.[18,19]  Both these spectroscopic properties are extremely sensitive to changes in the rhombicity at the ferric ion.

In nitrimyoglobin, the conjugated system of the $b$-heme is extended by chemical addition of a nitro group to one of the vinyl substituents.[20]  The UV−visible spectrum is significantly perturbed, but low-spin ferric derivatives give rise to EPR and NIR MCD spectra which are typical for analogous derivatives of normal myoglobin.[11]

These two examples involve an *extension* of the porphyrin conjugated system which is in contrast to chlorins where it has been condensed, but they still serve to illustrate that in such *delocalized* systems the loss of macrocycle $\pi$-symmetry is not necessarily reflected in significant increases in rhombicity at the ferric ion.

This work will show that low NIR-CT MCD intensities can actually result from more fundamental differences in the electronic character of low-spin ferric ion in porphyrins and
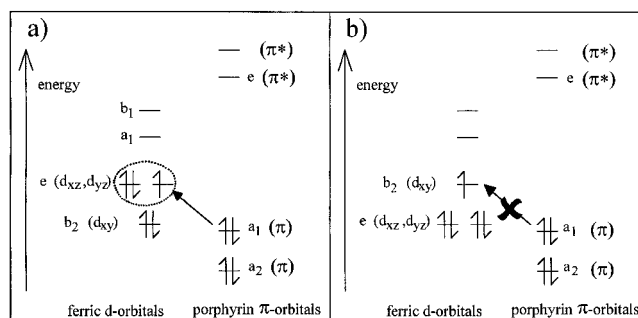
(13) Sutherland, J.; Greenwood, C.; Peterson, J.; Thomson, A. J. *Biochem. J.* **1986**, *233*, 893−898.

(14) Thomson, A. J.; Gadsby, P. M. A. *J. Chem. Soc., Dalton Trans.* **1990**, 1921−1928.

(15) Caughey, W. S.; Smythe, G. A.; O'Keefe, D. H.; Maskasky, J. E.; Smith, M. L. *J. Biol. Chem.* **1975**, *250*, 7602−7622.

(16) Vanderkooi, G.; Stotz, E. *J. Biol. Chem.* **1965**, *240*, 3418−3424.

(17) van der Oost, J.; de Boer, A. P. N.; de Gier, J.-W. L.; Zumft, W. G.; Stouthamer, A. H.; van Spanning, R. J. M. *FEMS Microbiol. Lett.* **1994**, *121*, 1−10.

(18) Eglinton, D. G.; Johnson, M. K.; Thomson, A. J.; Gooding, P. E.; Greenwood, C. *Biochem. J.* **1980**, *191*, 319−331.

(19) Cheesman, M. R.; Watmough, N. J.; Pires, C. A.; Turner, R.; Brittain, T.; Gennis, R. B.; Greenwood, C.; Thomson, A. J. *Biochem. J.* **1993**, *289*, 709−718.

(20) Bondoc, L.; Timkovich, R. *J. Biol. Chem.* **1989**, *264*, 6134−6145.

**Figure 1.** One-electron energy level scheme for low-spin ferric heme illustrating the porphyrin ($\pi$) → ferric ($d$) near-infrared charge-transfer (NIR-CT) band. The transition is (a) allowed and $xy$-polarized for a pure $(d_{xy})^2(d_{xz},d_{yz})^3$ ground state but (b) symmetry-forbidden for a pure $(d_{xz},d_{yz})^4(d_{xy})^1$ ground state. The orbitals are labeled according to $D_4$ symmetry.

chlorins.  Evidence is presented that the unusual $(d_{xz},d_{yz})^4(d_{xy})^1$ ferric ion electronic ground state can alone lead to reduced NIR-CT band intensities.  Such a ground state is consistent with the unusual EPR spectra of the type observed for low-spin ferric chlorins.  These results were obtained not using ferric chlorins but with a 4-fold symmetric ferric *porphyrin* in combination with appropriate axial ligands.  Thus, the chlorin structure appears to favor a ferric $(d_{xz},d_{yz})^4(d_{xy})^1$ ground state, but is not a prerequisite for its occurrence.

In this work, three low-spin complexes of ferric tetramesitylporphyrin (Fe$^{III}$TMP), each representative of a limiting case electronic configuration, have been examined by using low-temperature MCD spectroscopy.  When non-encumbered hemes such as ferric tetraphenylporphyrinate (TPP) and ferric octaethylporphyrinate (OEP) are liganded by imidazoles or highly basic pyridines, the parallel ligand-plane conformation is significantly stabilized by the strong rhombic crystal field.[21,22] This raises the degeneracy of the $d_{xz},d_{yz}$ pair and the unpaired spin tends to become localized in the orbital of higher energy.  Rhombic type EPR spectra, with $g_1 \approx 2.9$, $g_2 \approx 2.2$, and $g_3 \approx 1.5$, result.[21]  For Fe$^{III}$TMP complexes, this still holds for unhindered imidazole ligands, but steric interactions between substituted pyridine ligands and the bulky (2,6-dimethylphenyl)-porphyrin substituents result in the perpendicular orientation being favored.[23,24]  Such an arrangement results in minimal rhombicity at the ferric ion and near-degeneracy of the $d_{xz},d_{yz}$ orbital pair, within which the unpaired spin is significantly delocalized.  These species give rise to large $g_{max}$ type EPR spectra in which $g_z \geq 3.3$.[21]  The other two $g$-value features are broad and often difficult to detect.  In the theoretical axial limit, where the $d_{xz},d_{yz}$ orbitals are isolated and degenerate, the $g$-values of the EPR spectrum would approach 4,0,0.  In this limit, illustrated in Figure 1a, the NIR-CT transition is $xy$-polarized and gives rise to maximal MCD intensity.  As rhombicity is introduced to such a system, the electron-hole is progressively localized in one of the now non-degenerate $d_{xz},d_{yz}$ orbitals.  The NIR-CT transition becomes more $x$- or $y$-polarized and the MCD intensity is reduced.  In reality the presence of spin−orbit coupling precludes the occurrence of the limiting axial system and an effective upper limit of $g_z \sim 3.88$ is observed.

The complex [Fe$^{III}$TMP(4-NMe$_2$Py)$_2$]ClO$_4$ (**1**) has almost perpendicularly orientated ligand planes (79°) in the solid state

(21) Walker, F. A.; Huynh, B. H.; Scheidt, W. R.; Osvath, S. R. *J. Am. Chem. Soc.* **1986**, *108*, 5288−5297.

(22) Walker, F. A.; Simonis, U. *Encyclopedia of Inorganic Chemistry*; King, R. B., Ed.; John Wiley & Sons: New York, 1994; Vol. 4, pp 1817−1820.

**Table 1.** EPR and MCD Properties of Low-Spin Ferric TMP Complexes

| Fe$^{III}$TMP(L)$_2^+$ | EPR $g$-values | | | Taylor coefficients ($c_i$) | | | | $(C_{ct}/D_{ct})^g$ | zeroth moment of NIR-CT band | | | linear correction$^h$ | $\Delta\epsilon^*/\epsilon^i$ obsd |
| | $g_z$ | $g_y$ | $g_x$ | $a(d_{yz})$ | $b(d_{xz})$ | $c(d_{xy})$ | $\Sigma c_i^2$ | | $\Delta\epsilon^*/\epsilon^i$ calcd | MCD ($\Delta\epsilon_0$) $\int(\Delta\epsilon/\nu)\,\delta\nu$, dm$^3$ mol$^{-1}$ cm$^{-1}$ | absorption ($\epsilon_0$) $\int(\epsilon/\nu)\,\delta\nu$, dm$^3$ mol$^{-1}$ cm$^{-1}$ | | |
|---|---|---|---|---|---|---|---|---|---|---|---|---|---|
| (**1**) L = 4-NMe$_2$Py | 3.38 | ±1.91 | ±0.36$^a$ | 0.84 | 0.48 | 0.25 | 1.00 | 1.4558 | **1.16** | | | | |
| | 3.44 | ±1.80 | ±0.92$^b$ | 0.89 | 0.43 | 0.15 | 1.00 | 1.3446 | **1.08** | | | | |
| | 3.32 | | $^c$ | | | | | | | 67.6 | 95.3 | 1.35 | **0.96** |
| (**2**) L = 1-MeIm | 2.886 | 2.325 | 1.571$^d$ | 0.97 | 0.24 | 0.14 | 1.01 | 0.682 | **0.55** | | | | |
| | 2.90 | 2.33 | 1.52$^c$ | 0.96 | 0.25 | 0.15 | 1.01 | 0.7146 | **0.57** | 49.9 | 97.2 | 1.32 | **0.68** |
| (**3**) L = 4-CNPy | −1.56 | ±2.53 | ∓2.53$^e$ | 0.18 | 0.18 | 0.96 | 0.99 | −0.780 | **−0.62** | | | | |
| | −(1.42) | ±2.57 | ∓2.57$^{c,f}$ | 0.21 | 0.21 | 0.94 | 0.98 | −0.710 | **−0.57** | 7.35 | 63.5 | 1.20 | **0.14** |

$^{a,b}$ Set 1 (*a*) and set 2 (*b*) from fits of Mössbauer data for *crystalline* sample in ref 21. Only a $g = 3.48$ feature was observed in the EPR spectrum. $^c$ Frozen DMF/acetonitrile solutions used in this work. $^d$ Frozen CH$_2$Cl$_2$ solutions in ref 21. $^e$ Solid state EPR results in ref 22. $^f$ Only $g = 2.57$ observed. $g = 1.42$ is estimated from $\Sigma g_i^2 = 15.2$. See text. $^g$ Calculated from $C_{ct}/D_{ct} = g_z ab/[a^2 + b^2] = 2ab[(a + b)^2 - c^2]/[a^2 + b^2]$. $^h$ Required correction to observed MCD moment to compensate for departure from *linear limit* at 4.2 K and 5 T. $^i$ $\Delta\epsilon^*/\epsilon$ is the *linear limit* value of $\Delta\epsilon/\epsilon$. The predicted value of $\Delta\epsilon^*/\epsilon$ calculated from the expression $\Delta\epsilon^*/\epsilon = (C_{ct}/D_{ct})(\mu_B B/kT)$, where $\mu_B$ is the Bohr magneton and $k$ is Boltzmann's constant. At $B = 5$ T and $T = 4.2$ K, $(\mu_B B/kT) = 0.800$. The "observed" value, $\Delta\epsilon^*/\epsilon$, is obtained by correcting the experimental quantity $\Delta\epsilon_0/\epsilon_0$ for non-linearity at 4.2 K and 5 T.

and is an example of a large $g_{max}$ type complex.[23] In [Fe$^{III}$-TMP(1-MeIm)$_2$]ClO$_4$ (**2**) the ligand planes are parallel and a rhombic EPR spectrum is observed[23] (4-NMe$_2$Py is 4-(dimethylamino)pyridine and 1-MeIm is 1-methylimidazole).

Low-basicity substituted pyridines, such as 3-ClPy and 3- and 4-CNPy, are very strong $\pi$-acceptors and are believed to stabilize the $d_{xz},d_{yz}$ orbitals to the extent that they drop in energy below the $d_{xy}$ orbital, in which the unpaired spin is then predominantly localized.[25] The $\pi$-acceptor axial ligands favor enhanced porphyrin → Fe$^{III}$ $\pi$-bonding. This is itself strengthened by near degeneracy of the $d_{xz},d_{yz}$ orbitals and these complexes are thus found with near-perpendicular ligand planes.[24,25] These systems therefore exhibit *axial* type EPR spectra with unusual $g$ values. The third complex examined is an example of this class. [Fe$^{III}$TMP(4-CNPy)$_2$]ClO$_4$ (**3**, 4-CNPy is 4-cyanopyridine) has perpendicular ligand planes and an EPR spectrum with $g_{xy} = 2.57$ and $g_z = 1.56$. It is an example of the putative $(d_{xz},d_{yz})^4(d_{xy})^1$ ground state.[24,25] Figure 1b illustrates the limiting case in which the unpaired electron is located in the non-degenerate $d_{xy}$ orbital. As this theoretical situation is approached, all three EPR $g$ values converge toward $g_e \approx 2$. Again, in practice, spin–orbit coupling prevents this from being achieved.

These three TMP complexes thus provide the opportunity to compare spectroscopically each type of $(d_{xy})^2(d_{xz},d_{yz})^3$ ground state both with the other and with the $(d_{xz},d_{yz})^4(d_{xy})^1$ ground state. Importantly, this is achieved using a single porphyrin system in which 4-fold symmetry of the $\pi$-network is maintained through the use of identical substituents at the four *meso* positions.

**Materials and Methods**

*N,N*-Dimethylformamide (DMF) and acetonitrile (both spectrophotometric grade), 1-methylimidazole (redistilled-grade), 4-(dimethylamino)pyridine, and 4-cyanopyridine were all purchased from Aldrich. Tetramesitylporphyrin was purchased from Mid-century. [Fe$^{III}$(TMP)-OClO$_3$] was synthesized as previously described.[23] For low-temperature MCD measurements, an optically transparent glass is required. This was achieved by preparing samples in a solvent mixture of DMF and acetonitrile (3:1 by volume). Spectroscopic samples were made by the addition of solutions of the ligands to solutions of [Fe$^{III}$(TMP)-

(23) Safo, M. K.; Gupta, G. P.; Walker, F. A.; Scheidt, W. R. *J. Am. Chem. Soc.* **1991**, *113*, 5497−5510.

(24) Safo, M. K.; Gupta, G. P.; Watson, C. T.; Simonis, U.; Walker, F. A.; Scheidt, W. R. *J. Am. Chem. Soc.* **1992**, *114*, 7066−7075.

(25) Safo, M. K.; Walker, F. A.; Raitsimring, A. M.; Walters, W. P.; Dolata, D. P.; Debrunner, P. G.; Scheidt, W. R. *J. Am. Chem. Soc.* **1994**, *116*, 7760−7770.

OClO$_3$] (both in DMF/acetonitrile) to produce the final concentrations of heme listed in the figure legends. All ligands were used at a concentration of 0.1 M. Porphyrin concentrations were determined by weighings of [Fe$^{III}$(TMP)OClO$_3$]. For low-temperature MCD spectra, concentrations and extinction coefficients are quoted after correcting for the contraction to 80% of room temperature volume which occurs on freezing to liquid helium temperatures.

Electronic absorption spectra were recorded using an Hitachi U-3200, an Hitachi U4001, or a Cary-17D spectrophotometer. EPR spectra were recorded with an ER-200D X-band spectrometer (Bruker Spectrospin plc) fitted with a liquid helium flow cryostat (ESR-9, Oxford Instruments) and interfaced to an ESP1600 computer. Magnetic circular dichroism spectra were measured using a split-coil superconducting solenoid, type SM-4 (Oxford Instruments), capable of generating a maximum field of 5 T, and either a circular dichrograph, JASCO J-500D, for the wavelength range 300−1000 nm, or a home-built dichrograph[5] for the range 800−2300 nm.

**Results**

In order to establish a connection between the EPR spectra and NIR MCD intensities of these complexes, a knowledge of the EPR $g$ values is necessary. Low-temperature EPR spectra for the three Fe$^{III}$TMP complexes **1**, **2**, and **3** include both solid state and frozen solution results.[23,24] Reported $g$ values are listed in Table 1 along with those taken from Figure 2 which shows the X-band EPR spectra at 10 K of the three complexes in frozen DMF/acetonitrile solutions as used in this work for low-temperature MCD measurements. The spectra show that all three complexes are low spin at this temperature. For **3**, a feature near $g = 6$ represents a trace of high-spin ferric heme.

The axial ligands of solid state [Fe$^{III}$TMP(4-NMe$_2$Py)$_2$]ClO$_4$ (complex **1**) were shown by X-ray crystallography to be almost perpendicular both to each other and to the heme plane.[23] The large $g_{max}$ type EPR spectrum of Figure 2a shows that this is maintained for the solutions of this complex used here. In the crystalline state, **1** shows a $g_{max} = 3.48$ but $g_x$ and $g_y$ could not be detected.[23] Good fits to the Mössbauer data for this complex could be obtained using either of two similar parameter sets.[23] The $g$ values from these two sets are included in Table 1. In frozen dichloromethane solution, the $g_{max}$ value of **1** undergoes a shift to 3.33, a value similar to that of 3.32 observed in Figure 2a. For both frozen solution samples, $g_x$ and $g_y$ were again unresolved.

In the solid state complex **2**, [Fe$^{III}$TMP(N-MeIm)$_2$]ClO$_4$, is reported to display several overlapping sets of rhombic type EPR spectra.[23] The crystallographic structure shows two molecules in the unit cell both with parallel ligand planes but with distinct orientations of those ligand pairs with respect to
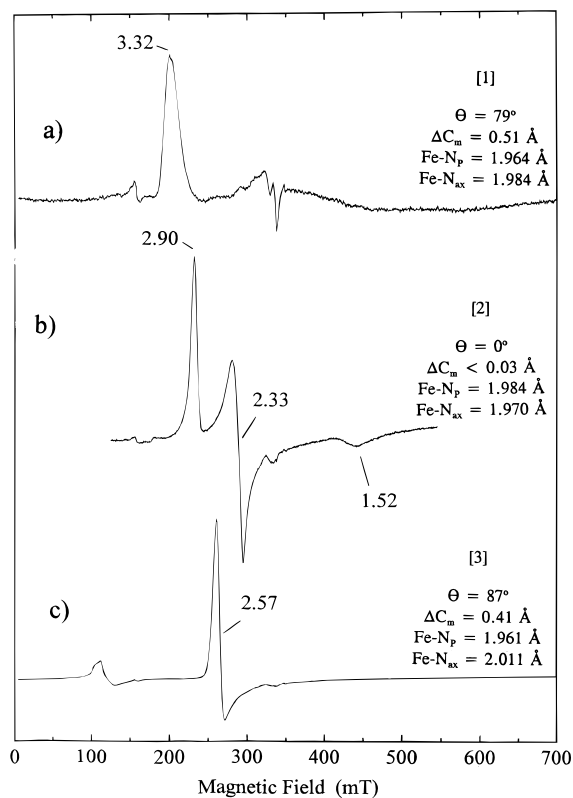
**Figure 2.** X-band EPR spectra of low-spin ferric TMP complexes in frozen DMF/acetonitrile (3/1 v/v) solutions: (a) 1.17 mM [Fe$^{III}$TMP-(Me$_2$NPy)$_2$]ClO$_4$ (**1**); (b) 1.13 mM [Fe$^{III}$TMP(N-MeIm)$_2$]ClO$_4$ (**2**); (c) 1.41 mM [Fe$^{III}$TMP(4-CNPy)$_2$]ClO$_4$ (**3**). Spectra were recorded at 10 K with 2.01 mW microwave power and 10 G modulation amplitude. Numbers given are as follows: dihedral angle between axial ligand planes ($\Theta$), average displacement of the meso-carbons from the mean plane of the porphyrin ($\Delta C_m$), Fe$-$N(porphyrin) bond length (Fe$-$N$_P$), and Fe$-$N(axial) bond length (Fe$-$N$_{ax}$).[23,24]

the porphyrin core. In frozen dichloromethane solution, **2** shows a single set of rhombic *g* values.[23] The frozen DMF/MeCN solution spectrum in Figure 2b shows a very similar spectrum (see Table 1).

The EPR spectrum of complex **3**, [Fe$^{III}$TMP(4-CNPy)$_2$]ClO$_4$, in frozen DMF/MeCN solution (Figure 2c) shows a $g_{x,y}$ feature at $g = 2.57$, similar to the $g = 2.53$ feature reported for this material in crystalline form.[24] No $g_z$ feature was resolved. In the crystalline spectrum, $g_z$ was observed at $g = 1.56$ giving $\Sigma g_i^2 = 15.2$. In Table 1, $g_z$ for the solution species has been estimated as 1.42 assuming that again $\Sigma g_i^2 = 15.2$. The EPR spectra of Figure 2 therefore establish that the forms of the complexes in the frozen solvent mixture used here are the same as those reported elsewhere and that comparison of reported physical properties is valid.

Figure 3 shows the room temperature UV$-$visible electronic absorption spectra of the complexes in the DMF/acetonitrile solvent mixture. Complexes **1** and **2** exhibit spectra typical of low-spin ferric hemes whereas complex **3** shows a broad structured Soret band and extra features near 630 and 700 nm. These are characteristics shared with [Fe$^{III}$TMP]ClO$_4$ in DMF/acetonitrile with no added ligand (Figure 3), which gives a low-temperature EPR spectrum characteristic of high-spin ($S = {}^5/_2$) ferric heme (not shown). Therefore, although the EPR spectrum of **3** shows it to be a low-spin species in a frozen glass at 10 K, the absorption spectra show that at room temperature in DMF/acetonitrile it exists as a mixture of high- and low-spin forms. However, the characteristic absorption spectra shown in Figure
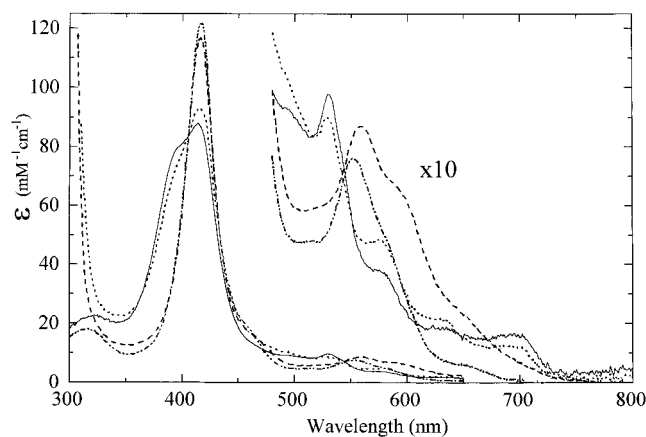


**Figure 3.** UV$-$visible region electronic absorption spectra of Fe$^{III}$-TMPClO$_4$ in pure acetonitrile at room temperature: ($-$) 95 $\mu$M [Fe$^{III}$-TMP]ClO$_4$; (---) 95 $\mu$M [Fe$^{III}$TMP]ClO$_4$ + Me$_2$NPy; (- · · -) 100 $\mu$M [Fe$^{III}$TMP]ClO$_4$ + N-MeIm; (···) 95 $\mu$M [Fe$^{III}$TMP]ClO$_4$ + 4-CNPy.
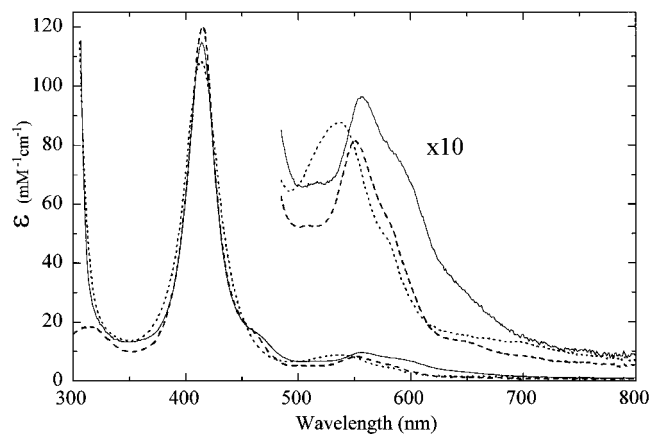


**Figure 4.** UV$-$visible region electronic absorption spectra of ferric TMP complexes in DMF/acetonitrile at room temperature: ($-$) 95 $\mu$M [Fe$^{III}$TMP(Me$_2$NPy)$_2$]ClO$_4$; (---) 150 $\mu$M [Fe$^{III}$TMP(N-MeIm)$_2$]ClO$_4$; (···) 140 $\mu$M [Fe$^{III}$TMP(4-CNPy)$_2$]ClO$_4$.
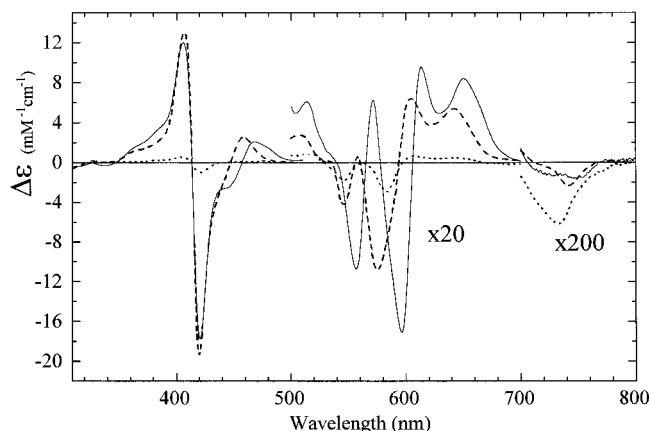


**Figure 5.** UV$-$visible region MCD spectra of low-spin ferric TMP complexes: ($-$) [Fe$^{III}$TMP(Me$_2$NPy)$_2$]ClO$_4$ (concentrations were 93 $\mu$M for 310$-$505 nm and 1.17 mM for 500$-$800 nm); (---) [Fe$^{III}$TMP-(N-MeIm)$_2$]ClO$_4$ (concentrations were 58 $\mu$M for 310$-$505 nm and 1.13 mM for 500$-$800 nm); (··) [Fe$^{III}$TMP(4-CNPy)$_2$]ClO$_4$ (concentrations were 68 $\mu$M for 310$-$505 nm and 1.41 mM for 500$-$800 nm). Spectra were recorded at 4.2 K with a magnetic field of 5 T.

4 indicate that, in pure acetonitrile, all three complexes are *low-spin* ferric hemes even at room temperature.

Figure 5 shows the UV$-$visible region MCD spectra of the three complexes in frozen DMF/acetonitrile. The spectra are shown only at 4.2 K, but all are strongly temperature dependent,
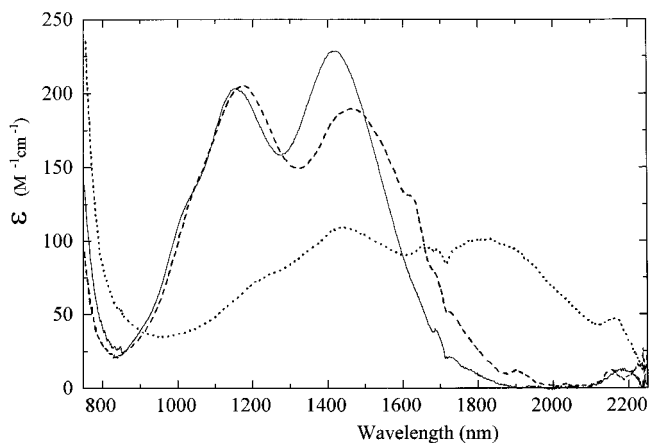
**Figure 6.** Near infrared region electronic absorption spectra of 4.76 mM ferric TMP complexes in DMF/acetonitrile at room temperature: (—) [Fe$^{III}$TMP(Me$_2$NPy)$_2$]ClO$_4$; (---) [Fe$^{III}$TMP(N-MeIm)$_2$]ClO$_4$; (···) [Fe$^{III}$TMP(4-CNPy)$_2$]ClO$_4$.



**Figure 7.** Near infrared region MCD spectra of low-spin ferric TMP complexes: (—) 1.17 mM [Fe$^{III}$TMP(Me$_2$NPy)$_2$]ClO$_4$; (---) 1.13 mM [Fe$^{III}$TMP(N-MeIm)$_2$]ClO$_4$; (···) 1.41 mM [Fe$^{III}$TMP(4-CNPy)$_2$]ClO$_4$. Spectra were recorded at 4.2 K with a magnetic field of 5 T.

consistent with a paramagnetic origin. Complexes **1** and **2** give rise to complicated spectra which contain intense derivative features corresponding to the Soret and to the α,β bands in the absorption spectra. The pattern of bands in these spectra is distinct from that found for low-spin ferric forms of octaethylporphyrin and of those hemes found in biological systems. The pattern of the features seen in Figure 5 and the wavelengths of these features are similar to those observed in the MCD spectra of complexes of low-spin ferric tetraphenylporphyrin (TPP) although the TPP complexes show a less pronounced MCD β band.[26] Both TPP and TMP have substituents on the methine bridges, whereas octaethylporphyrin (OEP) and protein-bound *b*- and *c*-type hemes lack substituents at these positions and in their low-spin ferric forms show α,β MCD bands which by comparison are red-shifted by approximately 30 nm.[26] The TPP-based complexes also show an additional positive MCD feature in the 640−660-nm region. A similar band is observed for the complexes of Figure 5.

The MCD intensities for complexes **1** and **2** are within the range observed for various low-spin ferric hemes with both patterns of substitution.[3,26] This is not so for the low-temperature UV−visible MCD of complex **3** shown in the same figure. While the band pattern of this spectrum is the same as those of complexes **1** and **2**, the intensities are substantially reduced.

Figure 6 shows the room temperature NIR electronic absorption spectra of the three complexes. These spectra were recorded at room temperature and in pure acetonitrile solvent in order to overcome difficulties associated with measuring a complete electronic absorption spectrum at 4.2 K. For an analysis of the low-temperature MCD intensities, it is necessary to have a measure of the dipole moment of the corresponding absorption spectra. Absorption spectra of the samples at 4.2 K in the MCD magnet cryostat have been recorded but these are not adequate for analysis for several reasons. It is not possible to obtain a true baseline for the spectrum recorded against a background which includes contributions from the liquid helium, several sets of quartz cryostat windows, and the variable nature of the frozen glass. Vibrational overtone bands occur across the NIR region[3] and cannot be referenced out of the low-temperature absorption spectrum whereas for room temperature solution work this is a fairly straightforward procedure. The spectra used for quantitation are therefore those of Figure 6 and
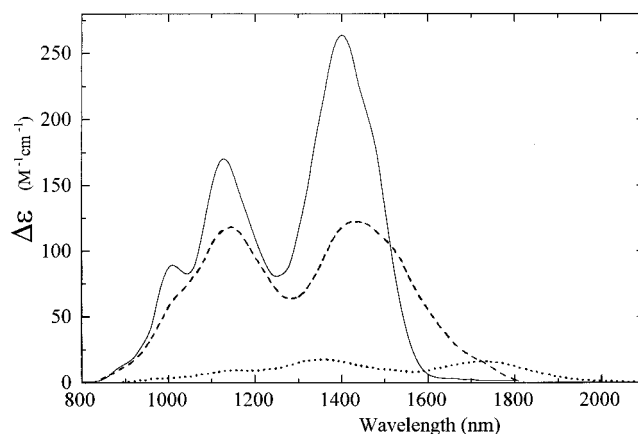
the zeroth moment of each absorption spectrum, $\epsilon_0 = \int (\epsilon/\nu)$ d$\nu$, is presented in Table 1. The low-wavelength limit used for each integration is the intensity minimum found between 800 and 1000 nm. In regions where the 4.2 K absorption spectra can be observed, peak to trough intensities adjusted for concentration differences agree with the spectra of Figure 6 to within 5%. The change from acetonitrile to DMF/acetonitrile solvent does not appear to significantly perturb the intensities. These two solvents have very similar dielectric constants.

The spectra of Figure 6 all show two major peaks with distinct structure. This pattern has also been observed in the MCD of low-spin ferric TPP complexes and it was suggested that the spectrum actually contains *two* porphyrin (π) → ferric (d) NIR-CT bands each showing vibrational side-structure.[26] Again this is a consequence of the different pattern of substitution, specifically that these porphyrins are substituted on the methine bridges unlike the biologically occurring hemes. However, the analysis of the CT bands below applies equally to one or both bands. The integrated NIR absorption intensity (Table 1) of complexes **1** and **2** are almost the same whereas that of **3** is significantly reduced.

The NIR MCD spectra of the three complexes at 4.2 K are shown in Figure 7. The pattern of bands in these spectra closely reflects those seen in the absorption spectra of Figure 6 but the relative intensities have altered substantially. The integrated MCD intensities, over the same energy range as performed for the absorption spectra, are shown in Table 1. The intensity for **2** is ∼74% of that of **1** but complex **3** shows an MCD spectrum an order of magnitude less intense. The following analysis attempts to correlate these MCD intensities with the EPR properties of the respective complexes.

**Analysis of Spectra.** The unpaired electron of a low-spin ferric heme can be described as occupying an orbital derived from the three non-σ-bonding d-orbitals (the T$_{2g}$ set in $O_h$ symmetry).[27] Table 1 shows the orbital coefficients of these three orbitals in the wave function of the unpaired electron as calculated from the *g* values using the model of Taylor,[28] in which it is argued that valid solutions require the determinant of the *g* tensor ($g_x g_y g_z$) to be a positive quantity for tetragonally distorted systems such as low-spin ferric hemes. The solutions given in Table 1 are those calculated in a "proper axis system", that is, a scheme which assigns the principal axes such that the *z*-axis is the direction of tetragonal distortion. Those listed for complexes **1** and **3** are unique solutions. The *g* values are all

(26) McKnight, J.; Cheesman, M. R.; Reed, C. A.; Orosz, R. D.; Thomson, A. J. *J. Chem. Soc., Dalton Trans.* **1991**, 1887−1894.

(27) Griffith, J. S. *Proc. R. Soc. London* **1956**, *A 235*, 23−36.
(28) Taylor, C. P. S. *Biochim. Biophys. Acta* **1977**, *491*, 137−149.

positive for **1** but for **3** $g(z,y,x) = (-1.56, 2.53, -2.53)$. The calculated orbital coefficients (*a, b, c*) for **3** are the basis for the proposition that such EPR spectra arise from low-spin iron-(III) porphyrin with a predominantly $(d_{yz}d_{xz})^4(d_{xy})^1$ ground state.

The solution for complex **2** listed in Table 1 also involves all positive g-values. However, a second solution within the Taylor criteria is possible for this complex, namely $g(z,y,x) = (-1.52, 2.33, -2.90)$. This results in orbital coefficients of (*a, b, c*) = (0.15, 0.25, 0.96), again a predominantly $(d_{yz}d_{xz})^4(d_{xy})^1$ ground state. However, for these rhombic type EPR spectra, the principal axis of the *g* tensor corresponding to the low-field *g* value is close to the heme normal,[29–32] and the $(d_{yz}d_{xz})^4(d_{xy})^1$ ground state is therefore unlikely. The analysis of the MCD data presented below clearly shows the $(d_{xy})^2(d_{xz},d_{yz})^3$ ground state assignment for complex **2** to be correct.

The formal electronic configuration of a typical low-spin ferric heme is $(d_{xy})^2(d_{xz}d_{yz})^3$ and the NIR-CT transition occurs from the porphyrin HOMO to the hole in the $(d_{xz},d_{yz})$ set. The model of Griffith more accurately describes the unpaired electron as occupying an orbital derived from the three non-$\sigma$-bonding d-orbitals (the $T_{2g}$ set in $O_h$ symmetry).[27] In the limit of high tetragonality and zero rhombicity, when the electron hole is distributed equally between the two (Figure 1a), the NIR-CT band is *xy*-polarized and the MCD is at its most intense.[14] In practice, a pseudo-Jahn−Teller distortion of the porphyrin opposes complete $d_{xz},d_{yz}$ degeneracy. Even for **1**, where the ligand planes are very nearly perpendicular, the $g_x$ and $g_y$ values are quite different.[23,29,33] With increasing rhombicity and loss of degeneracy of the $(d_{xz},d_{yz})$ pair, the hole becomes progressively localized in one of the two orbitals, leading to rhombic EPR spectra. The band then becomes predominantly *x*- or *y*-polarized depending on the orbital in which the electron is localized. Since linearly polarized transitions have no net MCD *C*-term intensity, the NIR-CT MCD band is substantially reduced in intensity. A range of low-spin ferric hemoproteins so far examined give rise to NIR-CT MCD bands the peak intensities of which vary at 4.2 K from $\Delta\epsilon \approx 580$ M$^{-1}$ cm$^{-1}$ [34] to less than 100 M$^{-1}$ cm$^{-1}$.[14] These values serve to illustrate the range of MCD intensities found for the NIR-CT band but, as will be described, it is the *intensity ratio* of the MCD to the absorbance which is governed by the symmetry. Implicit in this model is the assumption that the *z*-axis, defined under Taylor's "proper" axis system as the direction of tetragonal distortion, is perpendicular to the heme plane and therefore to the plane of the heme $\pi$-system.[28] This is indeed the case to within 15° in those hemes for which principal directions of the *g* tensor have been determined relative to molecular axes.[30–32,35]

These spectroscopic properties are common to the NIR-CT MCD band observed for the low-spin ferric state of *a*-, *b*- and *c*-type hemes.[3] They also apply to low-spin ferric octaethyl- and tetraphenylporphyrins (OEP and TPP), although, for the latter, the vibrational structure of the bands is variable. However, proteins containing low-spin ferric heme *d*, such as the cyanide derivative of Hydroperoxidase II (HPII) from *Escherichia coli* and octaethylchlorin (OEC) substituted myo-globin with a variety of low-spin ligands, give anomalously weak NIR-CT MCD bands with peak intensities of $\Delta\epsilon \leq 40$ M$^{-1}$ cm$^{-1}$.[10,12] The ground state electronic parameters calculated, *via* Taylor's treatment, from the EPR spectra of low-spin ferric hemes *d* show *low* rhombicity compared to *b*- and *c*-type hemes. These unusual EPR properties have led to suggestions that low-spin iron(III) chlorins have a predominantly $(d_{xz},d_{yz})^4(d_{xy})^1$ ground state.[28,36–38] An electronic transition from a porphyrin or chlorin HOMO to a hole in the $d_{xy}$ orbital is symmetry forbidden (Figure 1b) and therefore would have low intensity in both the absorption and MCD spectrum.

The low-spin ferric heme NIR transition involves a charge transfer between orbitals on different centers, namely the porphyrin $\pi$-orbitals and the ferric d-orbitals. It can only have non-zero intensity if mixing of orbitals occurs between the two centers. In the case of the heme system considered here, mixing can occur between the $4e(\pi^*)$ porphyrin orbitals and the metal $e(d_{xz},d_{yz})$ orbitals (Figure 1). It is assumed that the orbital *x*- and *y*-components mix to an equal extent characterized by a first-order mixing coefficient $\alpha$. Thus the $a_1,a_2$(porphyrin-$\pi$) $\rightarrow e(d_{xz},d_{yz})$ charge-transfer transitions borrow intensity from the $a_1,a_2$(porphyrin-$\pi$) $\rightarrow e(\pi^*)$ transitions which are responsible for the visible and Soret bands of heme spectra. The dipole strength of these $\pi-\pi^*$ bands is $D_{por} = {}^1/_3|m|^2$ where *m* is an electric dipole matrix element, $\langle a_1,a_2|m_x|e\rangle$, between the ground and excited states. The charge-transfer transition is allowed by symmetry to the $d_{xz},d_{yz}$ set but not to the $d_{xy}$ orbital. Consequently *a* and *b*, the Taylor coefficients for the contribution to the ground state from these two orbitals, appear in the final expression for the transition dipole moment of the CT transition,

$$D_{ct} = (1/3)\alpha^2(a^2 + b^2)|m|^2 \qquad (1)$$

At liquid helium temperatures, the MCD intensity is dominated by the *C*-term contribution. The magnitude of this *C*-term can be shown to be[14]

$$C_{ct} = (1/3)g_z ab\alpha^2|m|^2 \qquad (2)$$

These expressions already include averaging over all orientations of a randomly distributed powder sample. Thus the ratio of $C_{ct}$ to $D_{ct}$ is a quantity independent of $\alpha^2$ and $|m|^2$,

$$C_{ct}/D_{ct} = g_z ab/(a^2 + b^2) \qquad (3)$$

When the *C*-term is the only contribution to the MCD, the theoretical parameters $C_{ct}$ and $D_{ct}$ can be directly related to the experimentally observed parameters by

$$\Delta\epsilon^*/\epsilon = (C_{ct}/D_{ct})\cdot(\mu_B B/kT) \qquad (4)$$

where $\mu_B$ is the Bohr magneton, *B* is the magnetic field strength, *k* is Boltzman's constant, and *T* is the absolute temperature; $\epsilon$ is the absorption intensity and $\Delta\epsilon^*$ is the MCD intensity in the *linear limit*. To determine these two quantities, we have measured the zeroth moments, $\Delta\epsilon_0$ and $\epsilon_0$, of the bands in the respective experimental spectra:

(29) Quinn, R.; Valentine, J. S.; Byrn, M. P.; Strouse, C. E. *J. Am. Chem. Soc.* **1987**, *109*, 3301−3308.

(30) Hori, H. *Biochim. Biophys. Acta* **1971**, *251*, 227−235.

(31) Mailer, C.; Taylor, C. P. S. *Can. J. Biochem.* **1972**, *50*, 1048−1055.

(32) Byrn, M. P.; Katz, B. A.; Keder, N. L.; Levan, K. R.; Magurany, C. J.; Miller, K. M.; Pritt, J. W.; Strouse, C. E. *J. Am. Chem. Soc.* **1983**, *105*, 4916−4922.

(33) Soltis, S. M.; Strouse, C. E. *J. Am. Chem. Soc.* **1988**, *110*, 2824−2829.

(34) Rigby, S. E. J.; Moore, G. R.; Gray, J. C.; Gadsby, P. M. A.; George, S. J.; Thomson, A. J. *Biochem. J.* **1988**, *256*, 571−577.

(35) Helcké, G. A.; Ingram, D. J. E.; Slade, E. F. *Proc. R. Soc. London, Ser. B* **1968**, *169*, 275−288.

(36) Muhoberac, B. B.; Wharton, D. C. *J. Biol. Chem.* **1983**, *258*, 3019−3027.

(37) Muhoberac, B. B. *Arch. Biochem. Biophys.* **1984**, *233*, 682−697.

(38) Coulter, E. D.; Sono, M.; Chang, C. K.; Lopez, O.; Dawson, J. H. *Inorg. Chim. Acta* **1995**, *240*, 603−608.

$$\Delta\epsilon^0 = \int (\Delta\epsilon/\nu)\, d\nu \quad \text{and} \quad \epsilon_0 = (\epsilon/\nu)\, d\nu \quad (5)$$

Under the conditions of measurement, at 4.2 K and 5 T, the MCD is no longer linear with $1/T$. The measured moment $\Delta\epsilon_0$ is therefore corrected to give the higher value $\Delta\epsilon_0^*$, the *linear limit* MCD at 4.2 K and 5 T. The variation of the intensity of an $xy$-polarized MCD transition with temperature and magnetic field can be calculated for a spin $^1/_2$ system of known $g$ values following the methods developed previously.[39,40] Using this, the departure from linearity of the intensity at low temperature and high magnetic field can be calculated. The "linear correction" factors thus derived are shown in Table 1 for the various sets of $g$ values. Table 1 also shows the quantity $\Delta\epsilon^*/\epsilon$, the ratio of the MCD $C$-term to the electronic absorption dipole strength calculated from the EPR $g$ values for $T = 4.2$ K and $B = 5$ T. The observed value of this quantity is derived from the ratio of the zeroth moments of the MCD and absorption spectra of the NIR-CT band corrected for the loss of linearity of the MCD intensity at 4.2 K and 5 T. Because only $g_z$ was observed for **1** in frozen solution the calculated values of $\Delta\epsilon^*/\epsilon$ (1.16 and 1.08) are based on the $g$-value sets derived from the Mössbauer spectra of the crystalline material[23] and shown in Table 1. As can be seen from the table, the mathematical model is consistent with the spectroscopic properties of **1** and **2**, but fails to correlate the EPR $g$ values with the MCD properties of complex **3**.

## Discussion

For both model compounds **1** and **2**, which give rise to large $g_{max}$ and rhombic type EPR spectra, respectively, the observed quantity $\Delta\epsilon^*/\epsilon$ (Table 1) is in excellent agreement with the value calculated from the EPR $g$ values using the method of Thomson and Gadsby.[14] This illustrates clearly how the MCD intensity is derived from the absorption intensity but modulated according to the magnetic properties of the complex. This result, obtained using a particular ferric porphyrinate coordinated by similar ligands,[14] also underlines the central role of axial ligand orientation in determining EPR $g$ values and NIR MCD intensities. These measurements are frequently used to obtain information concerning the nature and orientation of ligands to hemes in proteins for which no three-dimensional structure is known. The results for complexes **1** and **2** constitute an important addition to the MCD data measured for low-spin ferric hemes of confirmed structure. These are necessary to endorse assignments of axial ligand orientation in hemoproteins made using this methodology.

The same analysis does not fully describe the properties of compound **3**, where the ligands are also known to be approximately perpendicular, a situation which confers effective 4-fold symmetry on the ferric ion, if the ruffling of the porphyrinate ring is ignored. Despite this 4-fold symmetry, the properties of **3** are distinct from those of **1**: The NIR MCD is extremely weak and the EPR spectrum is axial with $g$ values which suggest a reordering of the d-orbital energies leading to a formal $(d_{xz}, d_{yz})^4 (d_{xy})^1$ ground state. Since a charge-transfer process from either of the two highest occupied porphyrin $\pi$-orbitals to the hole in the ferric $d_{xy}$-orbital is symmetry forbidden, substantially reduced intensity would be anticipated for the NIR-CT band in both the electronic absorption and the MCD spectra of compound **3**. This is indeed true for the MCD band, which is approximately 11% of the intensity of the same MCD band for complex **1**. Direct comparison of the intensities

of equivalent MCD bands between complexes is of course only strictly valid if the mixing parameter $\alpha$ has a similar effect in each complex. However, it is interesting to note that the NIR-CT absorption intensity for **3** is as high as ~67% of the intensities for **1** and **2**. If the effect of $\alpha$ *is* comparable in all three complexes, then the absorption and MCD intensities would be proportional to $(a^2 + b^2)$ and $(g_z ab)$, respectively. On this assumption, an estimate can be made of the ratios of the absorption and MCD intensities of **3** to those of **1**. The predicted ratios are ~9% and ~5% compared to the observed values of 67% and 11% for the absorption and the MCD, respectively. The NIR-CT *absorption* intensity for **3** appears therefore to be anomalously high. We explore the possibility that this high absorption may result from the fact that the porphyrin ring of **3** is significantly deformed from planarity. The strong porphyrin $\rightarrow$ Fe$^{III}$ $\pi$-bonding in this and other related complexes leads to a shortening of the ferric ion to pyrrole nitrogen bonds. This is accommodated by a ruffling of the macrocycle.[24,25] An important aspect of such ruffling is the tilting of the individual pyrrole rings such that the ferric $d_{xy}$ orbital can have an effective overlap with the pyrrole−nitrogen $p_z$ orbitals. This allows delocalization of the unpaired spin onto the porphyrin *via* the $a_{2u}(\pi)$ orbital.[25] (A similar degree of ruffling is also observed for **1**, but in this case the electronic ground state is $(d_{xy})^2 (d_{xz}, d_{yz})^3$, and thus possible mixing of $d_{xy}$ with the porphyrin $a_{2u}$ orbital is not an issue.)

For **3** and other complexes with the "unusual" $(d_{xz}, d_{yz})^4 (d_{xy})^1$ ground state, mixing of porphyrin $a_{2u}$ with ferric $d_{xy}$ introduces $a_{1u} \rightarrow a_{2u}$ character into the NIR-CT band which, in the lower symmetry of the ruffled system, represents *linearly z-polarized* electric dipole intensity. This will invariably contribute to the absorption, but could also in principle add to the MCD intensity because the transition already has $xy$ character. The MCD intensity at 4.2 K is dominated by the temperature dependent $C$-term intensity and this is proportional to the expression[41]

$$g_x \langle a|m_y|j\rangle \langle j|m_z|a\rangle + g_y \langle a|m_z|j\rangle \langle j|m_x|a\rangle + g_z \langle a|m_x|j\rangle \langle j|m_y|a\rangle$$

$$(6)$$

where $a$ and $j$ are the ground and excited state wave functions. The residual $(d_{xy})^2 (d_{xz}, d_{yz})^3$ character of the ground state that results from spin-orbit coupling[27,28] is already contributing to the MCD *via* the third term of this expression. *Because the $g_x$ and $g_y$ values are equal in magnitude but of opposite sign, the first and second terms cancel and no net increase in MCD intensity results.* This is an important result, which accounts for the low intensity of the NIR-CT MCD bands while allowing the same bands in the *absorption* spectra to have reasonable intensity. Even if the values of $g_x$ and $g_y$ are not of *equal* magnitude, as in the rhombic spectra of the ferric chlorins reported to date,[28,36−38,42−44] they are in each case of *similar* magnitude and hence, with opposite sign, the first and second terms will *nearly* cancel in these cases.

An important conclusion from this work is that the novel "$d_{xy}$" ground state indicated by the unusual axial EPR $g$ values of compound **3** is in itself sufficient to result in anomalously low NIR-CT MCD intensities. This has important implications for

(39) Schatz, P. N.; Mowery, R. L.; Krausz, E. R. *Mol. Phys.* **1978**, *35*, 1537−1557.

(40) Thomson, A. J.; Johnson, M. K. *Biochem. J.* **1980**, *191*, 411−420.

(41) Piepho, S. B.; Schatz, P. N. *Group Theory in Spectroscopy with Applications to Magnetic Circular Dichroism*; Wiley: New York, 1983; pp 86−90.

(42) Dawson, J. H.; Bracete, A. M.; Huff, A. M.; Kadkhodayan, S.; Zeitler, C. M.; Sono, M.; Chang, C. K.; Loewen P. C. *FEBS Lett.* **1991**, *295*, 123−126.

(43) Gudat, J. C.; Singh, J.; Wharton, D. C. *Biochim. Biophys. Acta* **1973**, *292*, 376−390.

(44) Stolzenberg, A. M.; Strauss, S. H.; Holm, R. H. *J. Am. Chem. Soc.* **1981**, *103*, 4763−4778.

the interpretation of the magnetooptical spectra from proteins containing ferric hydroporphyrins. A "Taylor analysis" of the EPR $g$ values reported for low-spin ferric hydroporphyrins,[13,28,36–38,42–44] both in proteins and in model compounds, points to all these species having a predominantly $d_{xy}$ ground state. The few examples investigated by MCD spectroscopy to date give low UV−visible[45] and NIR-CT[11,12] intensities which have been interpreted as resulting from unusually high rhombicity at the ferric ion arising from the chlorin macrocycle.[11,12] On the basis of the arguments presented in the previous paragraph, this appears to be a misinterpretation; the $d_{xy}$ ground state itself leads to low NIR-CT MCD intensities.

The $d_{xz},d_{yz}$ orbitals are stabilized in **3** by use of strong $\pi$-acceptor axial ligands, resulting in the $(d_{xz},d_{yz})^4(d_{xy})^1$ ground state. In the absence of suitable axial ligands, the chlorin macrocycle itself may serve to provide this stabilization by more favorable $\pi^*-(d_{xz},d_{yz})$ interactions. Ruffling, which is believed to be easier for chlorins than for porphyrins,[46,47] would help this process. This ruffling would tend to lead to shorter M−N$_P$ bonds, thus facilitating the Fe $(\pi) \rightarrow$ chlorin $(\pi^*)$ back-bonding that would help to stabilize the $d_{xz},d_{yz}$ orbitals. Furthermore, ruffling would cause rotation of the $p_z$ orbitals of the chlorin nitrogens, just as it does for the porphyrins,[25] which can facilitate their overlap with the $d_{xy}$ orbital, thus mixing in the chlorin equivalent of porphyrin $a_{2u}$ character. Where rhombicity is observed in the EPR spectra of low-spin ferric chlorins, especially those bound in proteins, it may result from *either* axial ligand orientation *or* reduced macrocycle, *or both*. This work has examined the effect on the MCD of *one* of the several unusual properties of a ferric chlorin (the $(d_{xz},d_{yz})^4(d_{xy})^1$ ground state) and has shown that this one property is sufficient to reduce NIR-CT intensity to the level observed for actual low-spin ferric chlorins. It is not yet clear what additional influence is exerted by ligand orientation and by the chlorin ring itself. The EPR spectra of low-spin ferric chlorin model complexes with known perpendicular and parallel ligands would be of great value in clarifying this point. Interestingly, preliminary EPR investigations of bis-ligand complexes of iron(III) pyropheophorbide *a* methyl ester show that for L = N-MeIm, 4-NMe₂Py, 4-CNPy, and 2-MeImH, the EPR spectra of all complexes are rhombic and are all consistent with $(d_{xz},d_{yz})^4(d_{xy})^1$ ground states, yet the individual $g$ values are unique for each complex,[48] suggesting secondary effects due to axial ligand orientation and basicity for these low-spin iron(III) chlorin complexes. These and related complexes are thus interesting systems for detailed investigation by electronic absorption and MCD spectroscopy, some of which are now in progress.

**Summary.** This work has shown that low-spin ferric TMP complexes giving rise to limiting case "large $g_{max}$" and rhombic EPR spectra show variable NIR-CT MCD intensities which are consistent with the theoretical model described earlier.[14] This theoretical treatment was originally derived for a formal $(d_{xy})^2$-$(d_{xz},d_{yz})^3$ configuration,[14] and in its original form fails to describe the system with a predominantly $(d_{xz},d_{yz})^4(d_{xy})^1$ ground state. However, consideration of the effect of the opposite signs of $g_x$ and $g_y$[28] on the matrix elements of eq 6 largely accounts for the loss of NIR-MCD intensity in complex **3**. This loss in MCD intensity is thus evidence for such a ground state and so supports the assignment made from Taylor analysis of the EPR $g$ values.

The results importantly establish that disruption of $\pi$-orbital symmetry is not itself a prerequisite for these unusual properties: The $d_{xy}$ ground state can be stabilized in iron porphyrins by using weak $\sigma$-donor, strong $\pi$-acceptor axial ligands, while in iron chlorins it appears that the reduced macrocycle itself, with a variety of axial ligands, is sufficient to stabilize this electron configuration.[48] The influence of reduced macrocyclic symmetry is detected in the band pattern of the UV−visible spectra of both low-spin ferric chlorins and formyl-substituted porphyrins.[45,49,50] A 2-fold splitting of absorption and MCD bands is observed compared to the typical spectra of the equivalent porphyrin systems. The low-temperature UV−visible MCD spectra of compound **3** also exhibited low absolute intensities compared to compounds **1** and **2**. Similar UV−visible MCD intensities are seen for protein bound low-spin ferric chlorins.[10,45] It is likely that this reflects a reduced degree of mixing between the paramagnetic d-orbital configurations and the porphyrin/chlorin $\pi-\pi^*$ transitions which is necessary if these transitions are to take on the paramagnetic properties of the ferric ion.

(45) Bracete, A. M.; Kadkhodayan, S.; Sono, M.; Huff, A. M.; Zhuang, C.; Cooper, D. K.; Smith, K. M.; Chang, C. K.; Dawson, J. H. *Inorg. Chem.* **1994**, *33*, 5042−5049.

(46) Pfaltz, A.; Jaun, B.; Fässler, A.; Eschenmoser, A.; Jaenchen, R.; Gilles, H. H.; Diekert, G.; Thauer, R. K. *Helv. Chim. Acta* **1982**, *65*, 828.

(47) Barkigia, K. M.; Thompson, M. A.; Fajer, J.; Pandey, R. K.; Smith, K. M.; Vincente, M. G. H. *New J. Chem.* **1992**, *16*, 599.

(48) Shokhireva, T. K.; Raitsimring, A. M.; Walker, F. A. Unpublished results.

(49) Sono, M.; Bracete, A. M.; Huff, A. M.; Ikeda-Saito, M.; Dawson, J. H. *Proc. Natl. Acad. Sci. U.S.A.* **1991**, *88*, 11148−11152.

(50) Huff, A. M.; Chang, C. K.; Cooper, D. K.; Smith, K. M.; Dawson, J. H. *Inorg. Chem.* **1993**, *32*, 1460−1466.